# Three-dimensional shape profiling by projection of binary patterns: generated by a deterministic optimization approach

**Conference Paper** · August 2017

DOI: 10.1117/12.2275355

CITATION
1

READS
11

**4 authors**, including:

Antonio Muñoz
University of Guadalajara
**36** PUBLICATIONS **66** CITATIONS
SEE PROFILE

Adriana Silva
University of Guadalajara
**5** PUBLICATIONS **22** CITATIONS
SEE PROFILE

PROCEEDINGS OF SPIE

SPIEDigitalLibrary.org/conference-proceedings-of-spie

# Three-dimensional shape profiling by projection of binary patterns: generated by a deterministic optimization approach

Adriana Silva
Antonio Muñoz
Jorge L. Flores
Jesús Villa

SPIE.

# Three-dimensional shape profiling by projection of binary patterns: generated by a deterministic optimization approach

Adriana Silva[a], Antonio Muñoz[b], Jorge L. Flores[a], and Jesús Villa[c]

[a]Departamento de Electrónica, Universidad de Guadalajara, Av. Revolución 1500, 44840 Guadalajara, Jalisco, México.
[b]Departamento de Ingenierías, Universidad de Guadalajara, Av. Independencia Nacional 151, 48900 Autlán, Jalisco, México.
[c]Laboratorio de Procesamiento Digital de Señales, Unidad de Ingeniería Eléctrica, Universidad Autónoma de Zacatecas, Av. Ramón López Velarde 801, 98000 Zacatecas, Zacatecas, México.

## ABSTRACT

Three-dimensional shape profiling by sinusoidal phase-shifting methods is affected by the non-linearity of the projector. To overcome this problem, the defocused projection of binary patterns has become an important alternative to generate sinusoidal fringe patterns. In this paper, we present an efficient technique to generate binary fringe patterns where we use the symmetry and periodicity properties of binary-coded sinusoidal intensity. This reduces the search-space for the optimization problem. The patterns are projected out-of-focus to generate quasi-sinusoidal patterns, which can be used together with a phase-shifting algorithm to retrieve 3-D shape measurements. Simulations and experimental results show the feasibility of the proposed scheme.

**Keywords:** 3-D shape profiling, projection out-of-focus, binary fringe patterns, optimization.

## 1. INTRODUCTION

In the last years, fringe projection profilometry (FPP) has been increasingly used for measuring three-dimensional (3-D) object surfaces.[1,2] Most of the techniques employ phase-shifting interferometry (PSI) algorithms for profile retrieval.[3,4] Their experimental setup consists of a commercial video projector and a digital camera, which are used to project and acquire a sequence of phase-shifted sinusoidal fringe patterns.

We would like to remark that commercial video projectors have a non-linear intensity response which leads to the deviation of the captured fringe patterns from ideal sinusoidal waveform (gamma error); as consequence of such deviation, the accuracy decreases. To overcome this shortcoming, many approaches have been proposed. Some of them include the projection of fringe patterns distorted with values previously obtained by pre-calibrating the gamma,[5] the implementation of lookup-tables or iterative algorithms to compensate the phase error caused by the gamma,[6,7] and increasing the number of fringe patterns.[8] Unfortunately, the gamma value is given by each projector model and it actually changes over time.[9] For this reason, the described methods are not practical to correct phase error introduced by gamma response.

Another way to solve the gammas problem consists on generating sinusoidal fringe patterns by projecting and acquiring defocused binary patterns. When the projector is defocused, it performs as a low-pass Gaussian filter to smooth the binary patterns into quasi-sinusoidal ones. Several techniques for the generation of binary fringe patterns have been presented.[9–15] Lei and Zhang proposed the squared binary method (SBM) to generate sinusoidal patterns by the properly defocused projection of binary patterns,[9] if the defocusing level is not the appropriate, the presence of high-order harmonics could affect the measurement accuracy. To reduce this problem, different proposals based on the pulse width modulation (PWM) have been presented.[10–12] Wang and Zhang presented the binarization of sinusoidal fringe patterns using the Bayer dithering algorithm,[13] this technique was introduced to generate binary patterns with a wide fringe pitch. Dai et al. improved the Bayer dithering

Further author information: (Send correspondence to Adriana Silva)
Adriana Silva: E-mail: adriana.sm57@gmail.com

Infrared Remote Sensing and Instrumentation XXV, edited by Marija Strojnik, Maureen S. Kirk,
Proc. of SPIE Vol. 10403, 1040312 · © 2017 SPIE · CCC code: 0277-786X/17/$18
doi: 10.1117/12.2275355

technique by optimizing the binary patterns in the phase and intensity domains.[14,15] Lately, the generation of binary patterns for defocused projection, has been considered as an optimization problem, for which it is desired to find a solution that minimizes the phase error and is also computationally viable.

In this paper, we propose an efficient computational technique to generate binary fringe patterns. Based on the one-dimensional (1-D) analysis of $2^T$ solution space, we determine that the search space $2^n$ $(n = T/2)$ contains solutions which are very close to the exhaustive solution. This conforms a binary patch which is employed to generate a two-dimensional (2-D) binary patterns by employing the properties symmetry and periodicity of the sinusoidal waveform. The patterns are projected out-of-focus to generate quasi-sinusoidal patterns, which can be used together with a phase-shifting algorithm to retrieve 3-D shape measurements.

The remainder of this paper is organized as follows. In Section 2, we describe with some detail the theoretical basis of our proposal. In Section 3 and 4, numerical simulations and experimental results are presented, respectively. Finally, in Section 5, we present the conclusions.

## 2. METHOD

A typical 3-D shape measurement system based on a sinusoidal fringe projection is illustrated in Fig. 1. The setup consists of a personal computer to generate and process the fringe patterns, a digital light projector (DLP) which is used to project the software generated fringe patterns, a high-resolution charged-coupled device (CCD) camera that is employed to capture the fringe patterns modulated by the objects surface, and a flat plate for calibration.

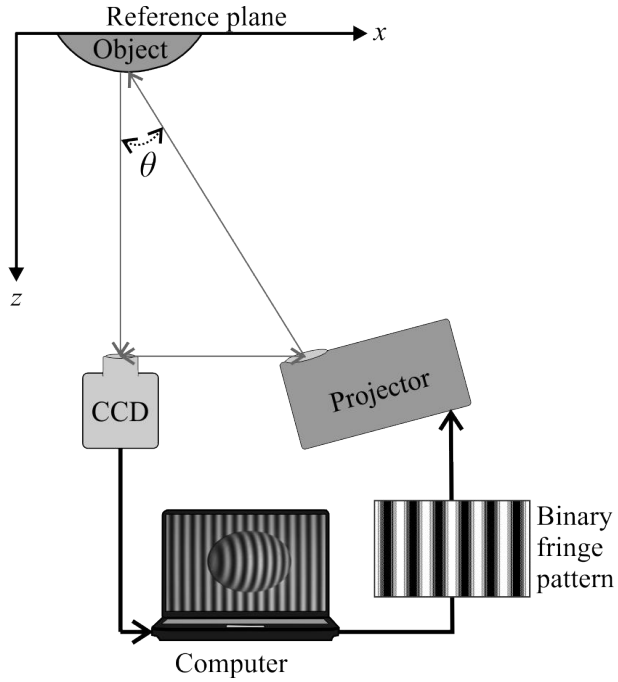


Figure 1. Experimental setup.

The three-step phase-shifting algorithm is widely used to calculate a wrapped phase map, because it only needs three fringe patterns. Considering that the phase step equals to $2\pi/3$, the intensity patterns can be described as

$$I_1(x,y) = A(x,y) + B(x,y)\cos[\phi(x,y) - 2\pi/3], \tag{1}$$

$$I_2(x,y) = A(x,y) + B(x,y)\cos[\phi(x,y)], \tag{2}$$

$$I_3(x,y) = A(x,y) + B(x,y)\cos[\phi(x,y) + 2\pi/3], \tag{3}$$

where $A(x,y)$ represents the background illumination, $B(x,y)$ is the amplitude modulation, and $\phi(x,y)$ is the phase to be determined. The wrapped phase can be estimated by

$$\phi(x,y) = \frac{\sqrt{3}[I_1(x,y) - I_3(x,y)]}{2I_2(x,y) - I_1(x,y) - I_3(x,y)}. \tag{4}$$

The Eq. (4) returns a wrapped phase whose values ranges are between $[-\pi, +\pi)$ with $2\pi$ discontinuities. In order to retrieve the continuous phase map an unwrapping phase technique should be applied.[16]

We would like to remark that, when the sinusoidal intensity fringe patterns are affected by the non-linear response of the projector, the previously described method does not work well. Thus, the defocused projection of a binary fringe pattern has become an alternative to overcome this problem.

### 2.1 Binary fringe patterns

When quasi-sinusoidal fringe patterns are generated by the technique of binary patterns out-of-focus projection, it is desired that the projected patterns be the closets to an ideal sinusoidal patterns. In this way, the procedure for the generation of binary patterns can be established as an optimization problem, mathematically described as

$$\min_{G,B} \|I(x,y) - G(x,y) * B(x,y)\|_2, \tag{5}$$

where $I(x,y)$ is the ideal sinusoidal fringe pattern, $G(x,y)$ is a Gaussian kernel, $B(x,y)$ is the binary fringe pattern, the symbol $*$ represents the 2-D convolution, and $\|\cdot\|_2$ denotes the L-2 norm. The above equation raises two unknowns $B(x,y)$ and $G(x,y)$. Also, the Eq. (5) represents a Non-deterministic Polynomial-time (NP) hard problem, therefore, it is impractical to solve it.

To generate the binary patter, we propose an alternative solution that is computationally efficient: we first generate a binary patch and then used it to create the binary pattern. In order to generate the binary patch, we reduced the solution space of Eq. (5) from 2-D to 1-D. In addition the optimization problem is concerned only about the binary pattern. Hence, Eq. (5) can be rewritten as

$$\min_{b} \|s(x) - g(x) * b(x)\|_2, \tag{6}$$

where the $s(x)$ is the sinusoidal pattern, $g(x)$ is the Gaussian kernel, $b(x)$ is the binary pattern to be optimized, and the symbol $*$ represents the 1-D convolution. Then, the stages to generate the binary pattern are the following:

1. Set the patch size in the $x$-direction. Which is equal to the desired fringe pitch ($P$). However, considering the symmetry property of a sinusoidal wavefront, during the optimization process we only look for an optimal solution to the half pitch ($T$), e.g. for a fringe pitch $P = 36$ pixels, $T = P/2 = 18$ pixels.
   In this stage, we also have to determine the size of the 1-D Gaussian kernel, e.g. $g = 5$ pixels with standard deviation ($\sigma$) of 5/3 pixels.

2. Find the binary values. By implementing an exhaustive search method we look for the optimal value to solve Eq. (6), but instead of searching in all the solution space $2^T$, we reduce the searching space to a sub-space $2^n$ where $n = T/2$, and complete the half pitch as follows

   $$b = \hat{b} + not[flip(\hat{b})], \tag{7}$$

   where $\hat{b}$ is the binary value searched in the sub-space $2^n$, $not[\cdot]$ represents the negation operator, and $flip(\cdot)$ indicates that the values of $\hat{b}$ are inversed in their position (as in a mirror). We would like to emphasize that the determination of Eq. (7), was obtained by analyzing several optimal values exhaustively, which were determined by taking into account several pairs of $\{n, b\}$ values. This strategy, reduces the search space in a half.

3. Complete the fringe pitch. By considering the symmetry property of a sinusoidal wavefront, we complete the binary pitch using the $b$ found. Then, we have to storage this binary array.

4. Find different solutions. We have to change the 1-D Gaussian kernel size, and repeat the Stages 2 - 4 using the same $T$. We suggest the use of five different Gaussian kernels, e.g. $g = m$ pixels with $\sigma = m/3$ pixels, where $m = 5, 7, 9, 11$ and 13.

5. Generate the binary patch. All the values stored in the Stage 3 are inserted in a different and consecutive row of the binary patch, observe Fig. 2 (b). In this way, the size of the binary patch in the $x$-direction is equal to $P$ pixels, while its size in the $y$-direction is equal to the number of kernels that have been used in the previous Stage.

6. Create the binary pattern. Considering the periodicity property of a sinusoidal wavefront, the binary pattern is created by repeating the patch pattern in the $x$ and $y$ direction many times as necessary (until complete the pattern size needed).

Our proposal is based on the observation that, if the optimal solution to Eq. (6) is found through exhaustive search in the solution space $2^T$, in almost all the cases, the binary solution has the form of the Eq. (7). One example of this is illustrated in Fig. 2.

In Figure 2 (a), the binary arrays indicated as $b_{o1}, b_{o2}, \ldots, b_{o5}$ are the optimal solutions to Eq. (6) found through exhaustive search in the solution space $2^T$, considering $T = 18$ pixels and using the five 1-D Gaussian kernel described in the fourth Stage. In Figure 2 (b), the binary arrays labeled as $b_{p1}, b_{p2}, \ldots, b_{p5}$ are the optimal solutions found by performing exhaustive search in the sub-space $2^n$, considering $T$ and the 1-D Gaussian kernel sizes as previously mentioned, and completing the half pitch as stated in Eq. (7). By comparing the solutions found in both cases, we can observe that the numerical solutions found are the same, except for the binary solutions identified as $b_{o5}$ and $b_{p5}$ which are obtained when $g = 13$ pixels with $\sigma = 13/3$ pixels. Their L-2 norm calculated was 0.0780 and 0.0881 for $b_{o5}$ and $b_{p5}$, respectively.

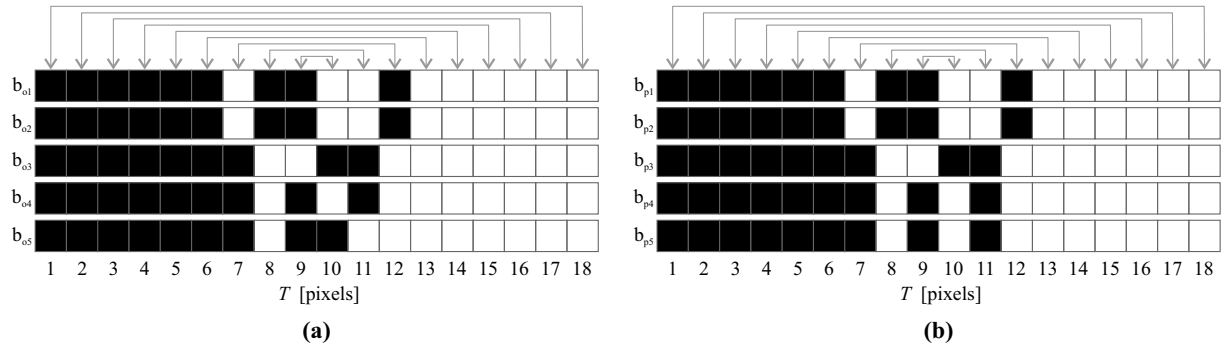


Figure 2. Binary arrays solutions of Eq. (6) considering $T = 18$ pixels; (a) Results obtained by performing exhaustive search in the solution space $2^T$. (b) Solutions obtained by exhaustive search in the solution sub-space $2^n$ and Eq. (7).

## 3. NUMERICAL SIMULATIONS

In this section, we conduct a series of computer simulations to test the performance of the proposed technique. First, we generated one binary pattern with a fringe pitch of 48 pixels (frequency of 22) and full size of $1056 \times 1280$ pixels (observe Fig. 3). Then, in order to simulate the defocusing effect, the binary pattern was smoothed by a low-pass Gaussian filter which was implemented as a convolution mask, to simulate different amounts of defocusing we used five 2-D low-pass Gaussian filters: $G_1 = 5 \times 5$ pixels with $\sigma = 5/3$ pixels, $G_2 = 7 \times 7$ pixels with $\sigma = 7/3$ pixels, $G_3 = 9 \times 9$ pixels with $\sigma = 9/3$ pixels, $G_4 = 11 \times 11$ pixels with $\sigma = 11/3$ pixels, and $G_5 = 13 \times 13$ pixels with $\sigma = 13/3$ pixels.

Figure 3 (a) shows the binary patch created by completing the Stages 1-5, where we set the fringe pitch equal to 48 pixels, and used the five 1-D Gaussian kernels suggested in the Stage 4. The blue rectangle encloses the binary values calculated. Figure 3 (b) shows the binary pattern created by repeating in the $x$ and $y$ direction the binary patch shown in Fig. 3 (a), which is also enclosed into the red rectangle.

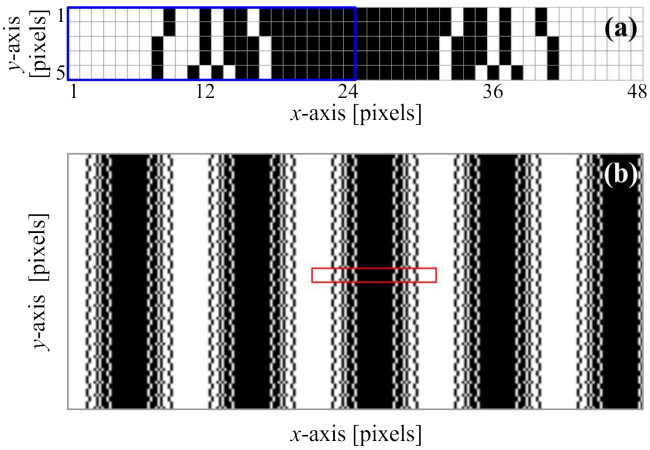


Figure 3. (Color online) (a) Binary patch and (b) Binary pattern, generated by the proposed method. Considering in both cases a fringe pitch of 18 pixels and five 1-D Gaussian kernels: $g_i = m$ pixels with $\sigma = m/3$ pixels ($i = 1, 2, \ldots, 5$ and $m = 5, 7, 9, 11, 13$).

Figure 4 (a) - (e) show an intensity visualization of a smoothed binary pattern with $G_1, G_2, \ldots, G_5$, respectively. Figure 4 (f) - (j) show a horizontal intensity cut of an ideal sinusoidal wavefront (black line), and the horizontal intensity cut (blue line) of the patterns shown in Fig. 4 (a) - (e), respectively. Figure 4 (k) - (o) show the phase difference between ideal sinusoidal fringe pattern and the smoothed patterns shown in Fig. 4 (a) - (e), respectively. We can observe that the intensity difference between the smoothed binary patterns and the ideal sinusoidal pattern, decreases as the 2-D low-pass Gaussian filter increases its size and its standard deviation, except when the pattern is smoothed with the $G_5$ filter.

In a second series of computer simulations, we tested the performance of the binary patterns for the three-step phase-shifting algorithm. As we already have the binary fringe pattern with initial phase of 0 rad, we utilized this to generate two more patterns shifted in phase by $-2\pi/3$ rad and $+2\pi/3$ rad, respectively. Then, the binary fringe patterns were smoothed using the previously described 2-D low-pass Gaussian filters ($G_1, G_2, \ldots, G_5$). After that, the smoothed patterns were used to retrieve the wrapped phase as it is indicated in the Eq. (4), and the unwrapped phase map was retrieved using the unwrapping algorithm described in Ref. 16. The phase error was measured as the root mean square (rms) error between these unwrapped phase maps and the unwrapped phase map retrieved from ideal sinusoidal fringe patterns. Finally, and thinking of simulating even more defocusing degrees, we smoothed the binary patterns by applying several times the smallest and the biggest ($G_1$ and $G_5$) 2-D low-pass Gaussian filters. Then we applied the procedure previously indicated to retrieve the unwrapped phase map and their rms error.

Figure 5 (a) shows the rms error obtained by smoothing the binary patterns with the 2-D low-pass Gaussian filters. As expected, we can observe that the higher rms error is obtained when the binary patterns are smoothed using the smaller filter, then as the filter size and its standard deviation increase, the rms error decreases. Figure 5 (b) shows the rms error calculated when the binary patterns were smoothed by applying them 1 to 8 times the $G_1$ and the $G_5$ low-pass Gaussian filters. In the first four iterations the rms error of the binary patterns smoothed by the $G_1$ filter is bigger than the rms error of the binary patterns smoothed by the $G_5$ filter. After this, the behavior changes, from the fifth iteration to the eight, in both cases the rms error tends to a constant value.

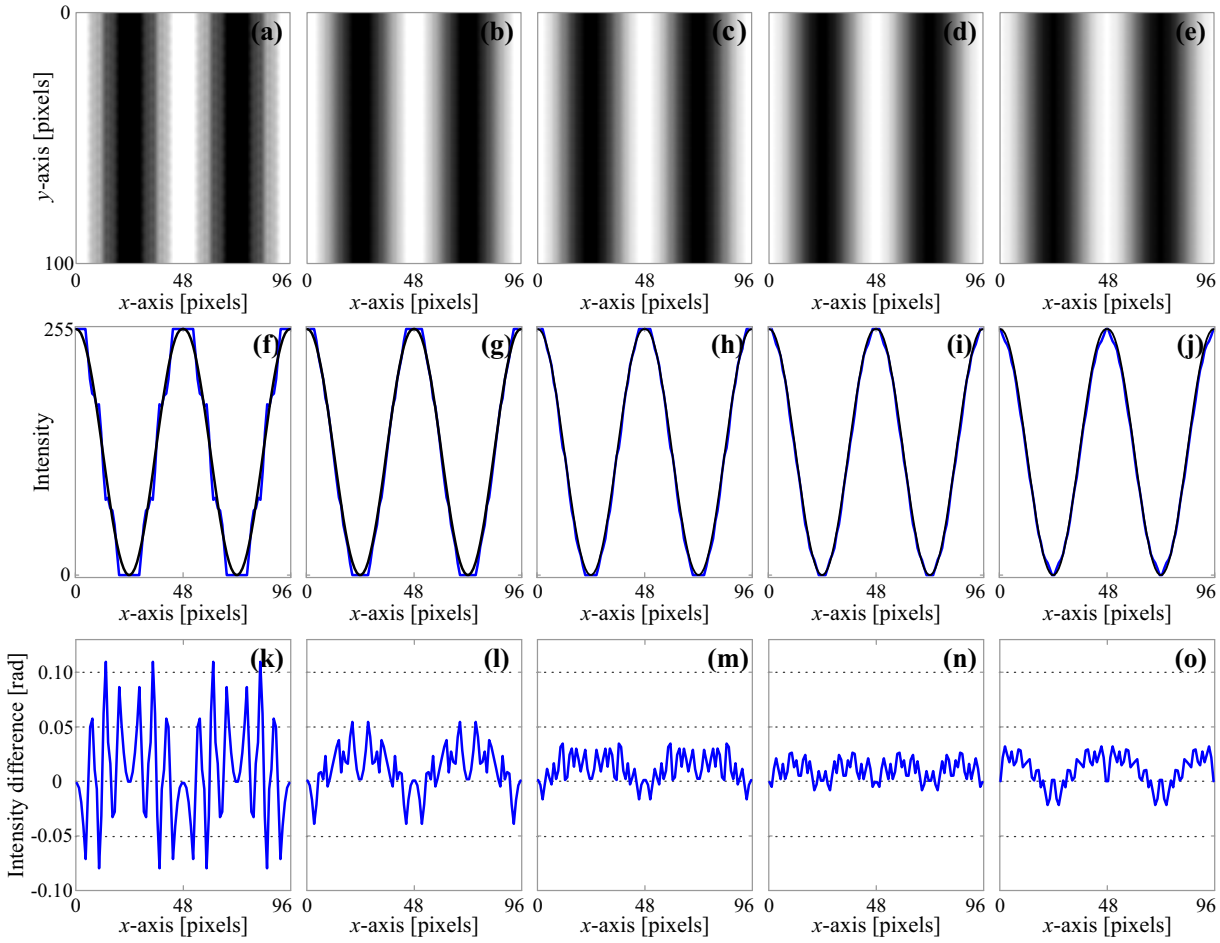


Figure 4. (Color online) (a) - (e) Intensity visualization of the binary patterns after being smoothed with: $G_1, G_2, G_3, G_4$, and $G_5$, respectively. (f) - (j) Black line: horizontal intensity cut of an ideal sinusoidal pattern, and blue line: horizontal intensity cut of (a) - (e), respectively. (k) - (o) Intensity difference between an ideal sinusoidal pattern and the smoothed patterns shown in (a) - (e), respectively.

## 4. EXPERIMENTAL RESULTS

We performed validation experiments by using a commercial LCD projector (model PJD7820, ViewSonic) with $1920 \times 1080$ pixels. The images were acquired with an 8 bit single-CCD camera (model DCU224C, Thorlabs) with $1280 \times 1024$ pixels, under a viewing angle of $\theta \approx 36$ deg.

In our first experiment, we proved the error introduced by the non-linearity of the projector. We projected and captured one sinusoidal fringe pattern, and we calculated its amplitude spectrum by the use of the fast Fourier transform (FFT). Then, over the same reference plane, we projected out of focus one of the binary patterns previously generated in the simulation, and we also applied the FFT to captured pattern in order to calculate its amplitude spectrum.

Figure 6 shows the amplitude spectrum of both patterns; sinusoidal in red line and defocused binary in blue line. We can observe that the FFT of the amplitude spectrum of the sinusoidal shows at least the first two harmonics in addition to the fundamental frequency. On the other hand, the spectrum of the defocused binary patterns does not contain these unwanted harmonics; therefore, the presence of harmonics in the Fourier spectrum confirmed the projectors non-linearity. We have verified as well that the proposed binary fringe patterns can have a quasi-sinusoidal waveform after being properly defocused.

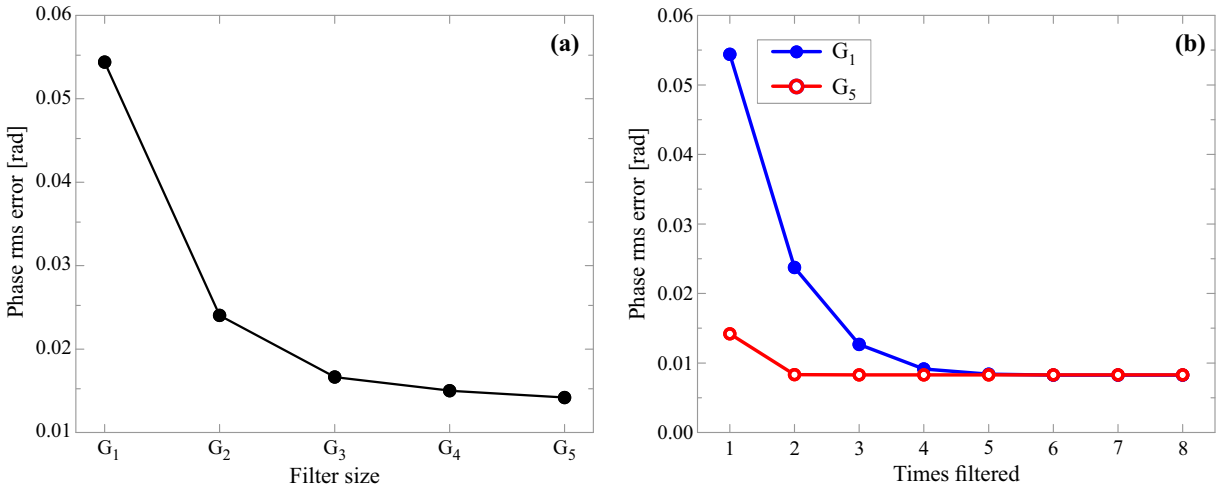


Figure 5. (Color online) Numerical simulation results; (a) Phase rms error obtained after having smoothed the binary patterns with five different 2-D low-pass Gaussian filters: $G_1 = 5 \times 5$ pixels with $\sigma = 5/3$ pixels, $G_2 = 7 \times 7$ pixels with $\sigma = 7/3$ pixels, $G_3 = 9 \times 9$ pixels with $\sigma = 9/3$ pixels, $G_4 = 11 \times 11$ pixels with $\sigma = 11/3$ pixels, and $G_5 = 13 \times 13$ pixels with $\sigma = 13/3$ pixels. (b) RMS error calculated after having applied 8 times the Gaussian filters $G_1$ and $G_5$.

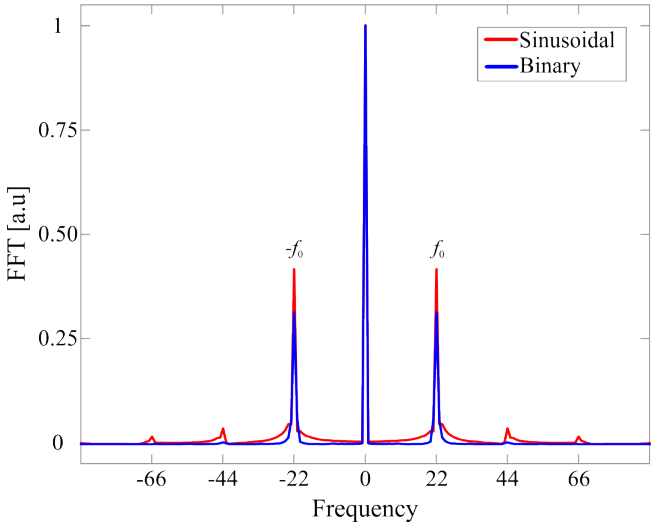


Figure 6. (Color online) Experimental results: FFT of the sinusoidal fringe pattern with pitch of 48 pixels (red line), and binary defocused fringe pattern with the same pitch fringe generated with our proposal (blue line).

In a second series of experiments, three binary fringe patterns previously generated were projected out of focus over a polystyrene semi-sphere, defocused in such a way that the captured fringe patterns were as close as possible to sinusoidal waveform as described in Eqs. (1) – (3). These patterns were used into Eq. (4) to retrieve the wrapped phase, and then the unwrapping phase was calculated using the method proposed by Ghiglia and Romero.[16] In order to compare our proposed method with the classical technique, we retrieved the objects phase profile by projecting/capturing sinusoidal fringe patterns without gamma correction and applying the same procedure previously described.

Figure 7 (a) – (b) show the 3-D object shape retrieved by projecting sinusoidal fringe patterns and defocused binary patterns, respectively. Figure 7 (c) – (d) show the intensity phase map of Fig. 7 (a) – (b), respectively. Figure 7 (e) – (f) show the cross section of the intensity phase maps depicted in Fig. 7 (c) – (d), respectively. We can observe that in both cases the intensity phase map shows a kind of ripples which can be produced by the

gamma error and by the noise. However, Fig. 7 (f) shows less error than the Fig. 7 (e), which clearly indicates that the proposed method is less sensible to those factors than the classical sinusoidal method.

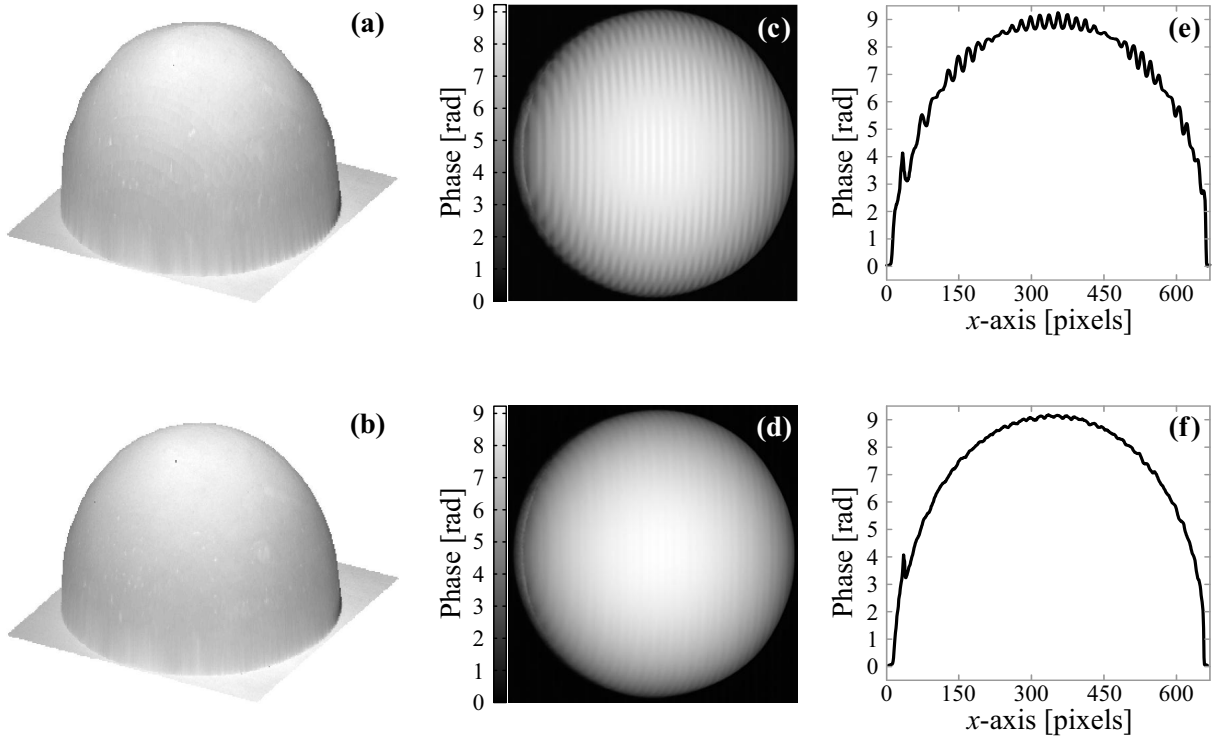


Figure 7. Experimental results: (a) – (b) 3D object shape retrieved by the implementation of three-step phase-shifting algorithm and the projection of: (a) sinusoidal patterns with fringe pitch of 48 pixels and frequency of 22, (b) defocused projection of the proposed binary pattern with the same fringe pitch and same frequency. (c) – (d) Unwrapped phase map of (a) and (b), respectively. (e) – (f) Horizontal phase profile of the phase map shown in (c) and (d), respectively.

## 5. CONCLUSIONS

In this paper, we have presented and efficient technique to generate optimized binary fringe patterns, which can be considered as quasi-sinusoidal patterns after being properly projected out-of-focus, and along with the phase-shifting algorithms, can be used to retrieve the 3-D profile of the surface of any given object. Our proposal defines an optimization heuristic based on the reduction of the solutions space used in the exhaustive search method, and in the properties of symmetry and periodicity of a sinusoidal waveform. With the proposed scheme, we can generate binary patterns where its pitch size is double to those that we could generate performing an exhaustive search method along with the symmetry property of the sinusoid (i.e. searching only in a half of the pitch). Furthermore, we showed numerical and experimentally, that the 3-D profile retrieved by the defocused projection of these optimized binary patterns is better than the 3-D profile generated by the projection of sinusoidal fringe patterns without gamma correction.

## REFERENCES

[1] Gorthi, S. S. and Rastogi, P., "Fringe projection techniques: whither we are?," *Optics and Lasers in Engineering* **48(2)**, 133–140 (2010).

[2] Geng, J., "Structured-light 3d surface imaging: a tutorial," *Advances in Optics and Photonics* **3(2)**, 128–160 (2011).

[3] Quan, C., Chen, W., and Tay, C. J., "Phase-retrieval techniques in fringe-projection profilometry," *Optics and Lasers in Engineering* **48(2)**, 235–243 (2010).

[4] Zhang, S., "Recent progresses on real-time 3d shape measurement using digital fringe projection techniques," *Optics and Lasers in Engineering* **48(2)**, 149–158 (2010).

[5] Peng, J.-Z., Ouyang, H.-K., Yu, Q., Yu, Y.-J., and Wang, K.-S., "Phase error correction for fringe projection profilometry by using constrained cubic spline," *Advances in Manufacturing* **2(1)**, 39–47 (2014).

[6] Zhang, S. and Huang, P. S., "Phase error compensation for a 3-d shape measurement system based on the phase-shifting method," *Optical Engineering* **46(6)**, 063601–063601–9 (2007).

[7] Pan, B., Kemao, Q., Huang, L., and Asundi, A., "Phase error analysis and compensation for nonsinusoidal waveforms in phase-shifting digital fringe projection profilometry," *Optics Letters* **34(4)**, 416–418 (2009).

[8] Huang, P. S., Hu, Q. J., and Chiang, F.-P., "Double three-step phase-shifting algorithm," *Applied Optics* **41(22)**, 4503–4509 (2002).

[9] Lei, S. and Zhang, S., "Flexible 3-d shape measurement using projector defocusing," *Optics Letters* **34(20)**, 3080–3082 (2009).

[10] Ayubi, G. A., Ayubi, J. A., Di Martino, J. M., and Ferrari, J. A., "Pulse-width modulation in defocused three-dimensional fringe projection," *Optics Letters* **35(21)**, 3682–3684 (2010).

[11] Wang, Y. and Zhang, S., "Optimal pulse width modulation for sinusoidal fringe generation with projector defocusing," *Optics Letters* **35(24)**, 4121–4123 (2010).

[12] Zuo, C., Chen, Q., Feng, S., Feng, F., Gu, G., and Sui, X., "Optimized pulse width modulation pattern strategy for three-dimensional profilometry with projector defocusing," *Applied Optics* **51(19)**, 4477–4490 (2012).

[13] Wang, Y. and Zhang, S., "Three-dimensional shape measurement with binary dithered patterns," *Applied Optics* **51(27)**, 6631–6636 (2012).

[14] Dai, J. and Zhang, S., "Phase-optimized dithering technique for high-quality 3d shape measurement," *Optics and Lasers in Engineering* **51(6)**, 790–795 (2013).

[15] Dai, J., Li, B., and Zhang, S., "High-quality fringe pattern generation using binary pattern optimization through symmetry and periodicity," *Optics and Lasers in Engineering* **52**, 195–200 (2014).

[16] Ghiglia, D. C. and Romero, L. A., "Robust two-dimensional weighted and unweighted phase unwrapping that uses fast transforms and iterative methods," *Journal of the Optical Society of America A* **11(1)**, 107–117 (1994).